Journal of Loss Prevention in the Process Industries 50 (2017) 154–164

Contents lists available at ScienceDirect

Journal of Loss Prevention in the Process Industries

journal homepage: www.elsevier.com/locate/jlp

Application and validation of the API analytical fire method in pressure-relieving and depressuring systems

Souvik Biswas*, Benjamin J. Fischer

Aspen Technology, Inc., Bedford, MA 01730, USA

ARTICLE INFO

Article history:
Received 10 August 2017
Received in revised form
14 September 2017
Accepted 17 September 2017
Available online 21 September 2017

Keywords:
Blowdown
Pressure vessel
Hydrocarbons
Fire
Simulation

ABSTRACT

Accounting for fire scenarios is critical when analyzing pressure-relieving and depressuring systems. This is particularly true in systems such as oil refineries, petrochemical facilities, gas plants, and oil and gas production facilities where the flowing fluids are highly flammable. Because operating safely is of paramount importance in these industries, standards and recommended practices have been developed by trade associations such as the American Petroleum Institute Standard 521 (API 521) to aid in the analysis of the system. In the case of fire scenarios, the traditional recommendation of API 521 has been an empirical model based on the wetted area of the vessel. However, in the most recent 6th edition released in 2014, the standard added an analytical equation based on the Stefan-Boltzmann law that can be used for modeling the dynamic response of pressurized vessels in fire scenarios. Using BLOWDOWN™ Technology in Aspen HYSYS, this analytical fire equation was validated with available experimental data and compared with the traditional wetted area model. This also included evaluating the effects of the parameters in the analytical equation such as surface emissivity of the equipment wall and external heat transfer coefficient, which have significant uncertainties. As plant fires can impact a wide area, this study further investigated using the analytical equation to model fire on a detailed geometry of a pressurized vessel with associated piping.

1. Introduction

Pressurized vessels exposed to fire in a hydrocarbon processing plant are an important area of investigation in the field of process safety. When a fire occurs in a plant, it is critical to evacuate the contents of any equipment in the vicinity in order to avoid escalation due to overpressure and potential catastrophic failure. A safe depressuring system should therefore be designed by including a careful analysis of fire scenarios. Often, this analysis can be performed using dynamic models. To be successful, the model must accurately represent the physical processes that occur inside the vessel as well as the physical nature of the fire.

During a depressuring event, a multiphase mixture of gas, liquid, and aqueous phases will flow through the vessel, valve, and any associated piping. As the fluid flows, there will be heat transfer between the fluid and vessel wall as well as between the different fluid phases. There will also be an accompanying mass transfer between the phases as liquid evaporates and vapor condenses. In addition, the fluid will follow a thermodynamic trajectory through the phase space that will often include phase changes and be close to or in the critical region. A simulation of this process must therefore predict the time-dependent pressures, temperatures and multi-phase compositions within a vessel, temperatures of the wall, and rates of efflux. Haque et al. (1992a) built a rigorous model to study these issues. Their computer program BLOWDOWN accurately captures both the thermodynamic behavior of the multi-component fluid inside the pressurized vessel and the heat transfer between the external thermal environment, the vessel wall and the internal fluid. The results were experimentally validated under cold conditions by tests conducted at Imperial College, London and the British Gas facilities (Haque et al., 1992b). This technology is now part of the general-purpose process simulation tool Aspen HYSYS.

Another important consideration is deciding how to model the behavior of the fire. Specifically, a model needs to be chosen for how the additional heat flux from the external fire is applied to the equipment. For example, the heat flux of a pool fire can be significantly different from that of a jet fire. Traditionally, to design a pressure relieving system to mitigate the risk of a fire hazard, standard industry practice for modelling the fire is to use the

* Corresponding author.
E-mail address: Souvik.Biswas@aspentech.com (S. Biswas).

https://doi.org/10.1016/j.jlp.2017.09.008
0950-4230/

American Petroleum Institute Standard 521 (API 521) pool fire equation. This is an empirical equation for the additional heat flux that should be applied to the liquid phase of the system. Consequently, this method is not recommended for determining the temperature response in the walls. To analyze the wall temperatures and potential rupture of a cylindrical vessel that is fully-engulfed by a fire, Mahgerefteh et al. (2002) simulated blowdown by modeling the fire as a constant heat flux to the outer wall of a vessel. As a constant heat flux model may not capture all of the physics of the fire and could be overly conservative, Salater et al. (2002) and the Scandpower Risk Management AS (2004) recommended modeling the fire with the Stefan-Boltzmann equation for thermal radiation along with the convective heat transfer from the hot gases to the vessel. These recommendations also introduced the approach of using a global average heat flux with a local peak heat flux to account for the spatial and temporal variability associated with any real fire.

As previously mentioned, there is some experimental data in literature on scheduled depressurization cases (Haque et al., 1992b) that has been used to validate depressuring models under cold conditions. Validating models for emergency depressurization scenarios where a vessel is under fire is challenging due to a lack of experimental data. However, there is data in the literature (Moodie et al., 1985, 1988) that examines the fire engulfment of LPG tanks. This data is used in the present study to validate the API analytical fire equation using the BLOWDOWN Technology in Aspen HYSYS. Subsequently, several case studies of emergency depressurization of vessels under fire attack are presented to compare the traditional API equation with the API analytical fire equation as well as to investigate the effects of the adjustable parameters in the API analytical fire equation. Finally, a more detailed geometry that includes process piping is investigated in order to examine the effects of local peak heat fluxes.

2. Fire modelling using API 521

To size an orifice associated with a blowdown valve used for emergency depressuring in a hydrocarbon processing plant, an accurate model of how much heat will be absorbed from the fire is required. Currently, the standard practice among safety engineers is to follow the American Petroleum Institute Standard 521 for pressure relieving and depressurizing systems. In the traditional API empirical equation, the total heat absorbed is a function of the wetted area given by:

$$Q = C_1 F A_w^{C_2} \tag{1}$$

$$C_1 = \left.\begin{array}{ll} 43.2 & (\textit{with drainage and firefighting}) \\ 70.8 & (\textit{without drainage and firefighting}) \end{array}\right\}, C_2 = 0.82$$

where

Q = heat absorbed by the liquid inside the vessel [kW]
A_w = wetted area [m^2]
F = environmental factor

As explained earlier, this heat is absorbed by the liquid inside of the vessel and is not applied to the vessel wall. Therefore, it should not be used to determine temperatures in the vessel wall nor is it applicable for unwetted vessels.

Due to the empirical nature of this model, it may not be applicable under all conditions. Roberts et al. (2004) found this approach to be non-conservative in cases of severe fires in offshore and in some onshore situations. Zamejc (2014) recommended a value of 1.0 for the factor C_2 when the vessel is partially confined by embankments or walls. Melhem and Gaydos (2015) found that this equation needs to be corrected by a fuel factor, which depends on the type of fuel as the emissive power of fire caused by lighter hydrocarbons is much greater than that by heavier hydrocarbons.

As mentioned earlier, Salater et al. (2002) and the Scandpower Risk Management AS (2004) provided a method on how to design such systems using the Stefan-Boltzmann radiation equation to model a fire. This method has since been incorporated into ANSI/API Standard 521 6th Edition (2014) as an alternative fire equation for designing for risk mitigation of a fire hazard in a process plant. Using this method, an additional heat flux to the outer wall of the vessel or pipe is determined rather than an additional heat flux to the liquid phase. The heat flux going into the fluid inside the vessel is then calculated by solving the heat transfer equations between the wall and the fluid inside the vessel. This heat flux is given by:

$$q_{absorbed} = \sigma\left(\alpha_s \varepsilon_f T_f^4 - \varepsilon_s T_s^4\right) + h(T_a - T_s) \tag{2}$$

where

$q_{absorbed}$ = absorbed heat flux by the vessel wall [W/m2]
σ = Stefan-Boltzmann constant [5.67×10^{-8} W/m^2-K^4]
T_f = fire temperature [K]
T_s = surface temperature [K]
T_a = ambient temperature [K]
ε_f = fire emissivity
ε_s = surface emissivity of the vessel wall
α_s = surface absorptivity of the vessel wall
h = heat transfer coefficient between surface and environment [W/m^2-K]

The main advantage Eq. (2) is that it is based on first principles; therefore, it has a much wider range of applicability and is not limited to pool fires or wetted vessels. In addition, given accurate inputs about the fire, it can be used to accurately predict wall temperatures of the vessel. Finally, it can be used to study the integrity of vessels and piping.

One potential issue of using Eq. (2) to model fire scenarios is that fires are often not uniform, which implies that there is not a uniform heat load from the fire to the vessel. To solve this issue, a recommended approach is to use a global average heat flux with a local peak heat flux (Scandpower Risk Management AS, 2004; ANSI/API Standard 521 6th Edition, 2014). The global average heat flux is the spatial and temporal average of the heat flux over the surface of the vessel. When multiplied by the vessel area, this is a good indicator of the total heat absorbed by the whole vessel over a period of time. Consequently, it is suitable for analyzing the pressure profile inside the vessel. The local peak heat flux is the maximum heat flux at a point in the vessel surface, which can be used to estimate the conservative transient temperature response of the vessel wall.

Another difficulty in applying Eq. (2) to a fire model is that the parameters are not commonly known during the design and sizing stage. To remedy this, API 521 provides ranges and default values for these parameters. However, as noted by Zamejc (2014), it is still possible to apply this equation incorrectly due to the many allowable permutations of these parameters.

3. Validation of fire engulfment of LPG tanks with experimental results

Presently there is a lack of published experimental data for a vessel undergoing emergency depressurization under fire. Most of the available experimental results of vessels exposed to fire are studies involving the fire engulfment of LPG tanks. The main purpose of these studies was to either evaluate the effectiveness of the pressure relief device protecting them or to estimate the time to failure of the vessel. Anderson et al. (1974) performed a detailed study of pool fire tests of a rail tank car filled with LPG. However, the liquid levels inside the tank during the tests were not reported. More recently, a full-scale pool fire test was conducted at the Federal Institute for Materials Research and Testing (BAM) in Germany (Balke et al., 1999; Ludwig and Heller, 1999). The main purposes of this test were to evaluate and compare fire exposure effects on a rail tank car containing propane and to measure the time required to reach the boiling liquid expanding vapor explosion (BLEVE) from fire ignition. In this time-to-failure test, full fire engulfment was not achieved due to prevailing wind conditions.

The previously mentioned experiments all lack some data that prevents a meaningful comparison with a model. However, tests carried out by the UK health and safety executive (Moodie et al., 1985, 1988) provide a complete set of data for the full fire engulfment of LPG tanks of several sizes (0.25 ton, 1 ton and 5 ton). The main objectives were to characterize the fire, determine the pressure increase inside of the vessel, and evaluate the operation of the pressure relief valves protecting the vessel.

These tests can be compared to simulations performed using the BLOWDOWN Technology in Aspen HYSYS, which is a general-purpose solver for determining the dynamic behavior of the multi-component fluids contained in a pressurized vessel. It accounts for both the thermodynamic behavior of the contents of the vessel and the heat transfer from the environment to the vessel. It can also be used to model fire scenarios using both the fire equations described in Eqs. (1) and (2).

When using Eq. (1) to model a fire scenario in BLOWDOWN, the heat is applied directly to the liquid inside the vessel. However, Eq. (1) also represents the total heat absorbed from the fire and API 521 does not give any guidance on how this total absorbed heat should be applied in a dynamic situation. In BLOWDOWN, it is assumed that the initial heat flux calculated by Eq. (1) with the initial wetted area remains constant over the duration of the dynamic simulation as shown in Fig. 1.

Alternatively, when using Eq. (2) to model a fire scenario in BLOWDOWN, the heat flux is applied to the outer surface of the vessel wall. As shown schematically in Fig. 2, the heat flux is initially the same in both the unwetted and wetted regions of the wall. However, the vapor wall temperature increases much faster than the liquid wall temperature because the heat transfer coefficient between the wall and the vapor inside of the vessel is very low. Therefore, the heat flux to the unwetted region of the wall decreases with time. Conversely, the heat flux to the wetted region will remain relatively constant.

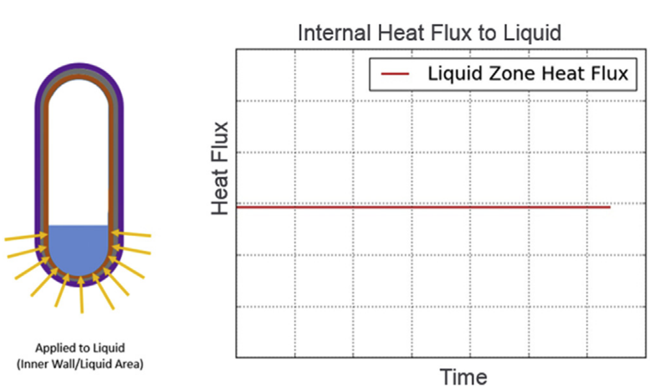

Fig. 1. The heat flux applied to the liquid phase as a function of time when using the empirical wetted area formula in API 521.

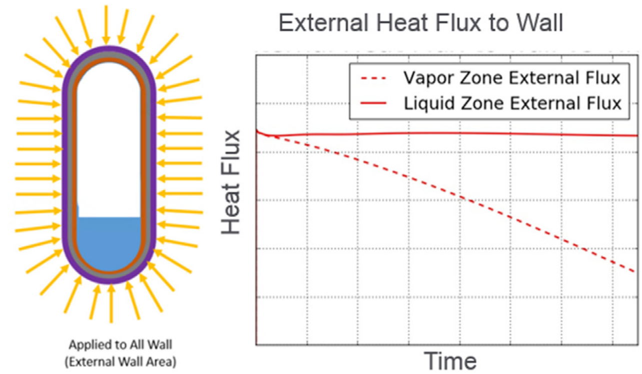

Fig. 2. Using the API 521 analytical fire equation, the heat flux is applied uniformly to the outside vessel wall, which leads to varying heat fluxes applied to each phase in the vessel as a function of time.

The use of Eq. (2) to model fire scenarios can be validated by comparing BLOWDOWN simulations with the fire engulfment tests on LPG tanks by Moodie et al. (1988). In this study, a 5 tonne LPG tank was fitted with two pressure relief valves with set pressures of 14.3 bar (gauge). Their operation was monitored to ensure that the pressure inside of the tank does not rise too high and cause a BLEVE explosion. The tank pressure was measured with pressure transducers at the top of the vessel where vapor is present and at the bottom where liquid is present. The overall accuracy of the pressure measurements was ± 0.1 bar. Tests were carried out with different liquid fill levels between 22% and 72% by volume. The tank was surrounded by three water tube calorimeters that were used to measure the heat flux from the fire and thirteen thermocouples were used to measure the bulk fluid temperature inside the vessel on two vertical planes. The total duration of fire exposure was 30 min.

Fig. 3 shows a flowsheet representation of the problem setup in BLOWDOWN. Because BLOWDOWN does not have a PRV but only a constant-diameter orifice model, the results can only be compared until the time when the PRVs protecting the vessels open. To simulate the period when the valves are closed, the orifice diameter

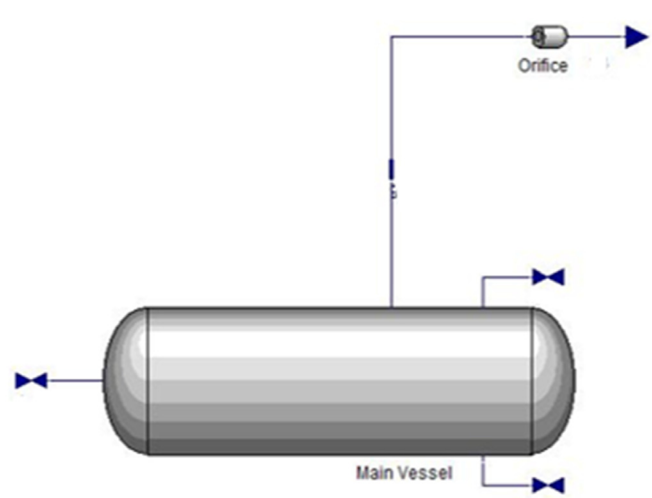

Fig. 3. Flowsheet representation of the LPG tank simulated with BLOWDOWN Technology in Aspen HYSYS.

was set to zero. Moodie et al. (1988) mentions that fire usually engulfed the whole vessel after 100–150 s after ignition and that the heat flux absorbed by the vessel was insignificant before the vessel was fully engulfed by fire. However, in the model, the fire flux must be applied from the beginning so the time is adjusted to reflect the time after fire engulfment.

To model the fire, the experimental fire heat flux data reported by Moodie et al. (1988) was averaged and then an initial heat flux was determined such that the same amount of total heat was added over the course of the simulation. In BLOWDOWN, the initial heat flux at time zero can be directly specified such that the fire temperature is back-calculated from Eq. (2). This fire temperature is assumed to be constant over time during the simulation. Based on the experimental data before the PSV opens for the first time, initial heat fluxes of 81.22 kW/m^2 and 75 kW/m^2 were used for the 72% liquid volume case and the 22% liquid volume case, respectively. Table 1 shows the parameters used for the analytical fire model for both the 22% and 72% case. The parameters like fire emissivity, surface emissivity, external heat transfer coefficient and hot gas ambient temperature were taken from the suggested default values for pool fire in API 521 Table A.3 (ANSI/API Standard 521 6th Edition, 2014). Table 2 shows the geometrical parameters used in the blowdown simulation and has been taken from Moodie et al. (1988).

During the fire engulfment experiment, the fluid temperatures were measured at thirteen fixed locations at different elevations on two vertical planes. In the 72% liquid fill case, there is only one location that consistently remained in the vapor zone. The top-most location where the temperature was measured was initially in the vapor zone. The temperature versus time curve for this location shows that this temperature initially rises rapidly and then decreases to merge with temperature curves of other locations which are known to be in the liquid zone (Moodie et al., 1988). This indicates that the liquid swells to this thermocouple level. The BLOWDOWN simulation for this case also shows that the liquid level rises with time. Fig. 4 shows the internal pressure and liquid temperature as a function of time for the 72% liquid fill case. Both pressure and temperature are a good match with the experimental data. It should be noted that BLOWDOWN determines different temperatures for the vapor and liquid phases in the vessel; however, it does not determine a spatial distribution within these phases but rather assumes a uniform temperature in each phase. The maximum error for pressure is found to be less than 0.8 bar and the maximum deviation in liquid temperature is less than 4C.

In the 22% liquid fill case, the top-most measurement locations for the temperature always remain in the vapor zone; therefore, the experimental temperature results for both the vapor and liquid phases can be compared to the experimental measurements. Fig. 5(a) shows the pressure rise inside the vessel with time. In this case, the BLOWDOWN results are found to be slightly higher and more conservative with the maximum error within 2 bar. Fig. 5(b) shows the temperature versus time data for both the vapor and liquid phases. The temperature results are slightly higher and more conservative for both phases with the maximum deviation within 9 C for the liquid temperature and within 13 C for the vapor temperature.

4. Depressurization case study: API wetted area equation VS. analytical equation

In the previous section, simulations using BLOWDOWN Technology in Aspen HYSYS were compared with experimental results obtained from fire engulfment studies of LPG tanks. Using the API analytical equation for fire, both the pressure and vapor and liquid temperatures inside the vessel were accurately predicted. A more complete study needs to investigate the effect of fire during a depressurization because this is often necessary when designing the size of a blowdown orifice. Because there is no experimental data for a comparison, a case study is performed using the “S13” case from Haque et al. (1992b) as BLOWDOWN has already been validated under ambient conditions for this situation. Table 3 provides the detailed information for the vessel parameters and Table 4 gives detailed information about the scenarios investigated.

Fig. 6(a) shows the pressure profile with time for all four scenarios. As expected, the rates at which the pressures decrease are slightly lower for the fire scenarios when compared to the case of ambient conditions. In addition, for all fire scenarios, the pressure profiles are similar initially. After approximately 600 s, the differences in the pressure profiles increase but not significantly.

Fig. 6(b) shows the liquid temperature inside the vessel for all four scenarios. It can be seen that the liquid temperature does not rise significantly during the simulation. This is due to the fact that most of the heat added to the liquid phase does not result in the sensible heating of the liquid. Instead, the heat added to the liquid is primarily used to provide the heat of vaporization to the liquid that evaporates into vapor. In the cases of the API wetted area equation (Scenario #3) and the API analytical equation with initial heat flux of 59.49 kW/m^2 (Scenario #4), the liquid inventory of the vessel completely vaporizes around 1000 s. Because the contents of the vessel are only vapor, a liquid temperature is not reported after this time in the simulation.

The vapor temperatures inside of the vessel and downstream of the orifice are shown in Fig. 6(c) and (d). Using the wetted area equation does not predict an increase in temperature of the vapor or the temperature of the fluid downstream of the orifice. As discussed, the heat applied to the liquid inventory inside the vessel primarily results in evaporation of liquid inventory. However, when using the analytical fire equation, heat is also transferred to the vapor phase. As a result, the vapor temperatures increase significantly, which could lead to a larger volumetric flow into the disposal or flare network. Fig. 7 shows the volumetric flow through the orifice when the flux calculated from the wetted area equation

Table 1
Input data for the 22% and 72% liquid fill by volume cases.

Parameters	72% Liquid case (by vol. %)	22% Liquid case (by vol. %)
Initial Heat Flux (kW/m^2)	81.22	75
Fire Emissivity	0.75	0.75
Surface Emissivity	0.75	0.75
Vessel Absorptivity	0.75	0.75
Ambient fire temperature (C)	600	600
External Heat Transfer Coefficient (W/m^2/C)	20	20
Fire Temperature (C)	942	914

Table 2
Input data for the 22% and 72% liquid fill by volume cases.

Parameters	72% Liquid case (by vol. %)	22% Liquid case (by vol. %)
Vessel Volume (m^3)	10.25	10.25
Vessel Diameter (m)	1.68	1.68
Head Type	Dished	Dished
Cylinder Wall Thickness (mm)	11.85	11.85
Head Wall thickness (mm)	18	18
Composition	LPG (C1: 0.06% C2:0.07% C3:94.96% C4:4.91%)	LPG (C1: 0.06% C2:0.07% C3:98.46% C4:1.40%)
Orifice Diameter (mm)	0.0	0.0
Final Time (s)*	206	253

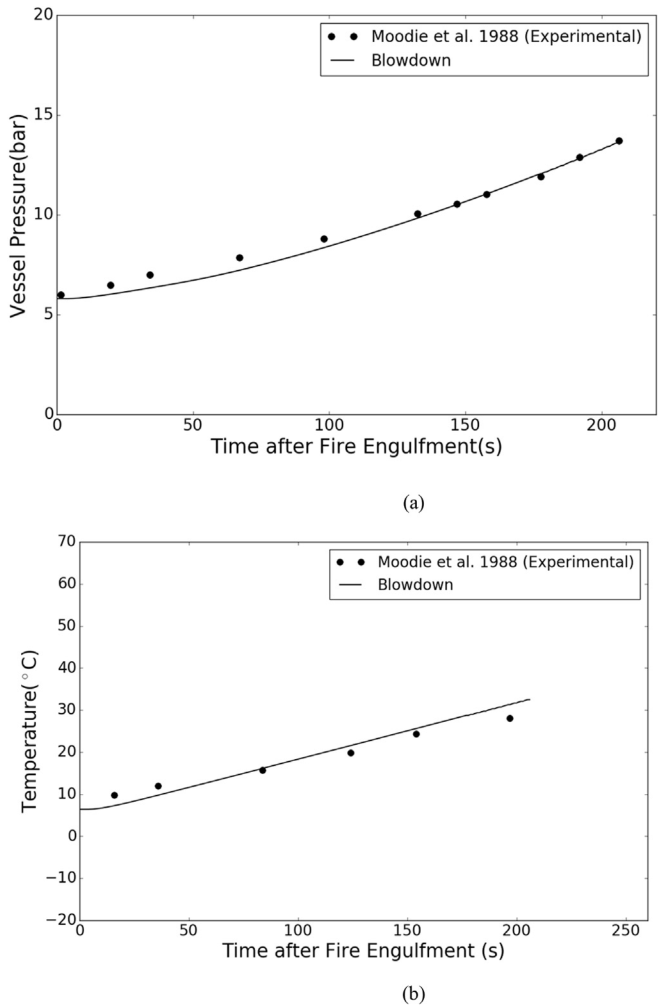

Fig. 4. Five tonne LPG tank (72% liquid by vol.): Evolution of the (a) pressure and (b) temperature of the liquid phase inside the vessel after fire engulfment.

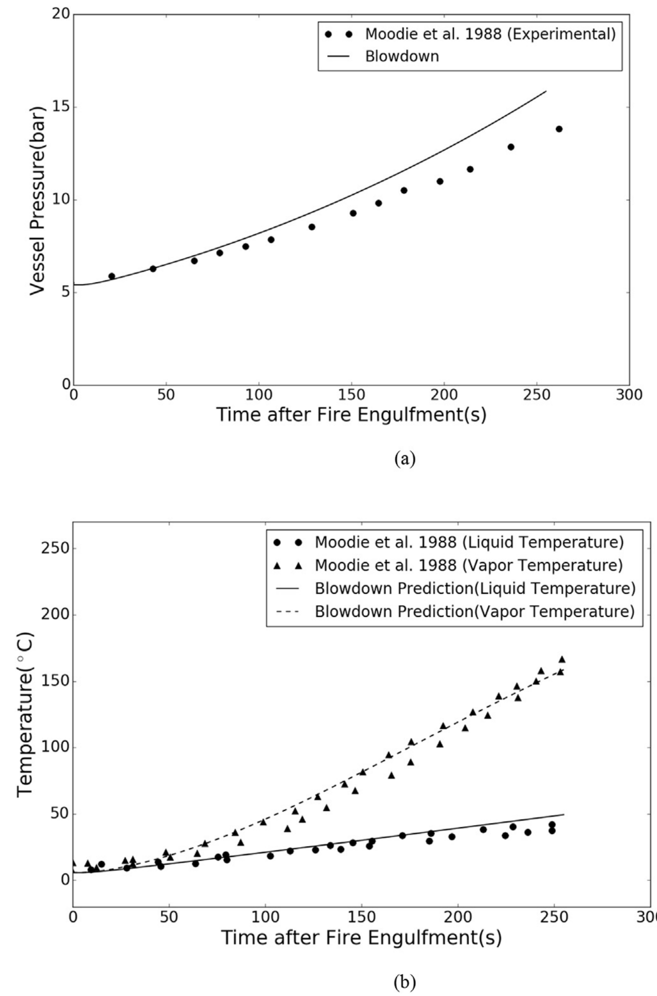

Fig. 5. Five tonne LPG tank (22% liquid by vol.): Evolution of the (a) vessel pressure and (b) temperature of the vapor and liquid phases inside the vessel after fire engulfment.

without drainage or firefighting (Scenario #3) and when the same flux was applied to the outside of the wall with the API analytical equation (Scenario #4). It can be seen that the volumetric flow rates are slightly elevated at the later stages of simulation with the analytical fire equation. This is mainly because the temperature of the vapor inventory is the same at earlier times for both the wetted area equation and the analytical equation. With the analytical equation, the vapor gradually heats up with time. However, it is not until the later stages of the simulation that the temperature of the vapor inventory is large enough to cause a noticeable change in the vapor volumetric flow rate. Although in this case the differences are marginal, this fact may be still be of some interest for safety engineers responsible for design of flare networks and staggered blowdown studies.

Zamejc (2014) pointed out that one of the drawbacks of the API analytical equation is that there are many possible permutations of input parameters like surface emissivity and external heat transfer coefficient. Therefore, using the analytical equation runs the risk of

Table 3
Vessel parameters used in the depressurization case study (Haque et al., 1992b).

Vessel Volume (m^3)	2.73
Vessel Diameter(m)	1.13
Head Type	Dished
Cylinder Wall Thickness (mm)	59
Head Wall thickness (mm)	50
Composition	C1: 66.5% C2: 3.5% C3: 30%
Liquid Amount	20%
Final Time (s)	1500
Orifice size(mm)	10

being wrongly applied, which has been an impediment for a wide-adoption of this method among safety engineers. Understanding the effect of various parameters can help guide the use of the analytical equation.

Experimental studies of fire engulfment have shown that fire temperature remains relatively constant with time for the duration of the fire (Anderson et al., 1974; Moodie et al., 1985, 1988). In most cases, wall temperature is the only parameter that is a function of time in the Eq. (2). As a result, the fire temperature can be calculated from the initial absorbed heat flux as was done earlier when performing the comparison with experimental results. Furthermore, the decrease in the heat flux to the system at later time, t, can be written as:

$$\Delta q_{absorbed} = q_{absorbed}|_{time=0} - q_{absorbed}$$

$$\Delta q_{absorbed} = \sigma \varepsilon_s \left(T_s(0)^4 - T_s(t)^4\right) + h(T_s(0) - T_s(t)) \tag{3}$$

Because the absorbed heat flux ($q_{absorbed}$) is the boundary condition for the system consisting of the vessel and the liquid and vapor inventory inside the vessel, the pressure and temperature profile of the vessel inventory with time only depends this condition. From Eq. (3), it can be seen that the decrease of this absorbed heat flux at a later time (t) only depends on the surface emissivity (ε_s) and the external heat transfer coefficient (h). This implies that if the initial heat flux ($q_{absorbed}|_{time=0}$) is fixed, then the absorbed heat flux boundary condition, and therefore the dynamic response of the vessel and its inventory will also depend only on these two parameters.

According to the API 521 guidance, the range of surface emissivity is between 0.3 and 0.8 (ANSI/API Standard 521 6th Edition, 2014, Table A.2). Using the value of surface emissivity and the default value for open fire of 45 kW/m^2 for the initial absorbed heat flux (ANSI/API Standard 521 6th Edition, 2014, Table A.3), the fire temperature can be calculated from Eq. (2). Fig. 8 shows the pressure profile and the vapor and liquid temperature profiles for different surface emissivity values of 0.3, 0.5, and 0.8 for the S13 case defined previously.

The convective heat transfer from the external hot gases surrounding the vessel is determined using the external heat transfer coefficient. For an open pool fire, the heat transfer coefficient is in the range of 10–30 W/m^2/°C (ANSI/API Standard 521 6th Edition, 2014, Table A.2). As above, the fire temperature is calculated such that the initial absorbed heat flux is 45 kW/m^2. Fig. 9 shows the pressure profile and the vapor and liquid temperatures for different external convective fluxes of 10, 20, and 30 W/m^2/°C.

It can be seen that if the initial absorbed flux is fixed, the profiles for the pressure and fluid temperatures are virtually the same even though the emissivity and heat transfer vary. In a vessel containing hydrocarbon liquid, the liquid inventory will absorb most of the heat from the fire, which causes the temperatures of the liquid and the wetted wall to increase. However, these temperatures will never reach a temperature higher than the bubble point of the hydrocarbon liquid. As a result, the decrease in heat flux to the wall at a later time, t, (i.e. $\Delta q_{absorbed}$) is very low compared to the initial heat flux ($q_{absorbed}|_{time=0}$) for hydrocarbon liquids. Therefore, neither the surface emissivity nor the external heat transfer coefficient has significant effects on either the pressure profile or the temperature in the case of the vessel containing liquid. As will be shown in the next section, this is not necessarily true in unwetted situations where the wall temperatures can get significantly higher.

5. Wall temperature analysis of a vessel with piping using a local heat flux

Dynamic simulation can be used to determine the required size of a blowdown orifice by analyzing the pressure response in a vessel under fire. However, in some hydrocarbon processing facilities (particularly offshore) there is a limitation in flare capacity, which imposes a constraint on freely sizing the blowdown orifice. For such cases, providing passive fire protection of critical process segments is suggested to protect the vessels and other process piping segments from failure (Salater et al., 2002). In a real fire case, the heat load from the fire to the vessel or process equipment is non-uniform. The pressure profile inside the vessel depends on the average heat load in such a case. However, the process equipment and piping can experience significant thermal weakening in an isolated spot due to a local peak heat flux, which can result in mechanical failure (Salater et al., 2002; ANSI/API Standard 521 6th Edition, 2014). To capture the effect of thermal weakening in a simulation, a local peak heat flux is applied to a specific location that is a small fraction of the total area exposed to the fire. Then, the transient behavior of the wall temperature at this location can be obtained. This can be used to determine whether the temperature rise is enough to weaken the wall material substantially and cause rupture. In a real fire, there is no guarantee that the peak heat flux impacts just one location during the whole depressurization. However, this is the most conservative way of designing for fire cases.

To apply this approach, it is necessary to study the detailed geometry of the process equipment under fire instead of a lumped volume. Fig. 10 shows a schematic diagram of the system investigated in which a vessel is connected by a pipe to the blowdown valve. It is also connected with a blocked outlet valve through

Table 4
Fire scenarios applied to S13 case.

Scenario #1	Scenario #2	Scenario #3	Scenario #4
No External Fire Flux	API analytical equation with initial heat flux to vessel wall = 45 kW/m^2 (API default for Open Fires, Table A.3)	Heat Flux directly to the liquid = 59.49 kW/m^2 (This value is calculated from API wetted area equation without drainage and firefighting. BLOWDOWN, assumes that the initial heat flux calculated initial wetted area remains constant over the duration of the dynamic simulation.)	API analytical equation with initial heat flux to vessel wall = 59.49 kW/m^2 (Flux obtained from API wetted area equation was applied to wall instead of applying to the fluid directly)

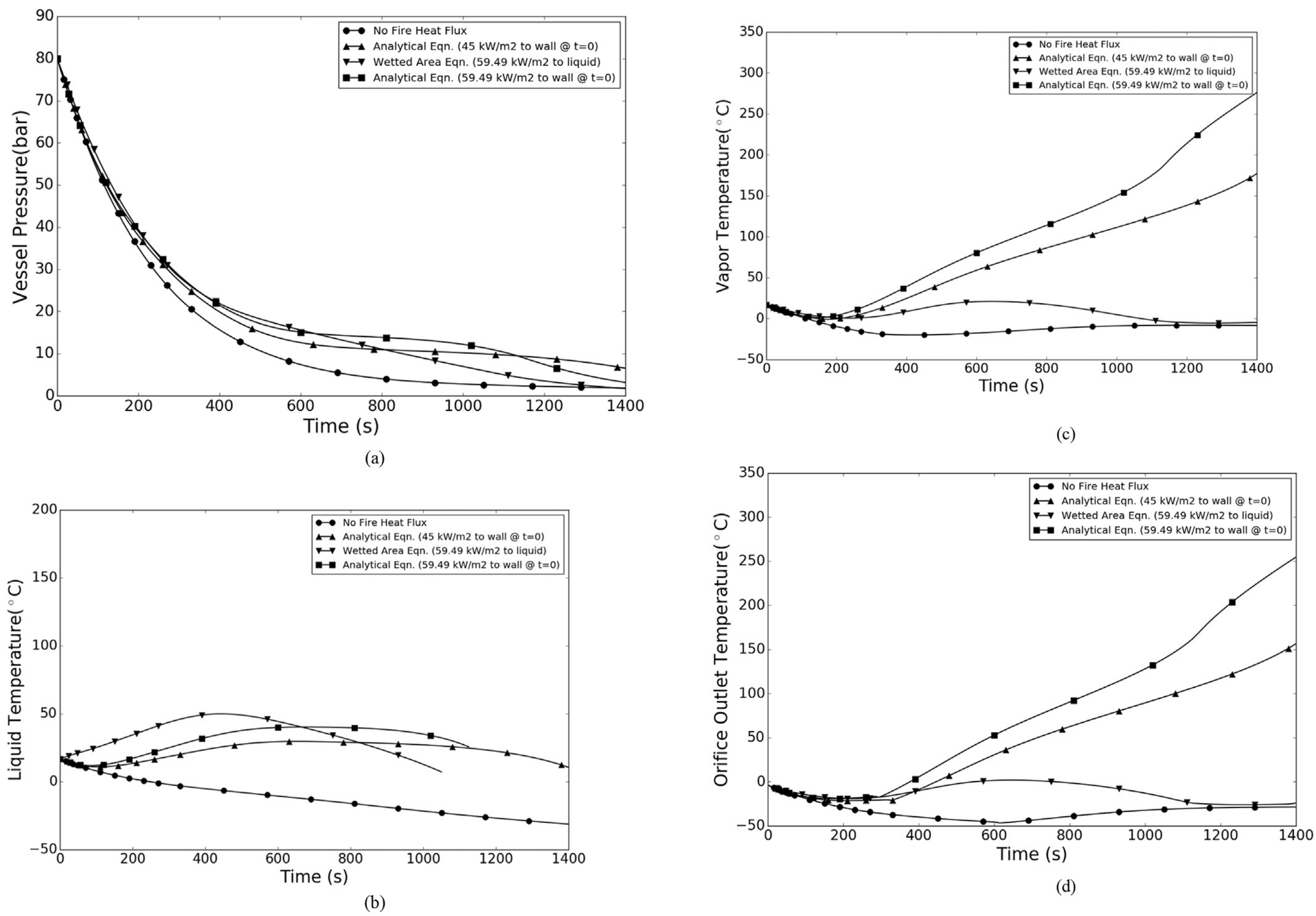

Fig. 6. S13 depressurization case (20% liquid inventory by vol.): Evolution of the (a) vessel pressure, (b) liquid temperature, (c) vapor temperature, and (d) fluid temperature at the orifice outlet with time for different fire loads.

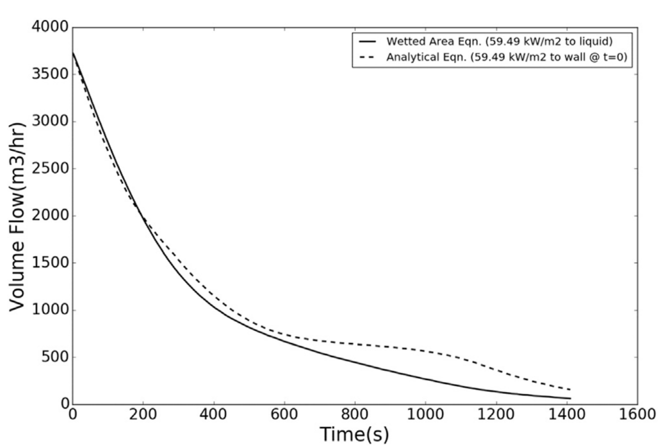

Fig. 7. S13 depressurization case (20% liquid inventory by vol.): Volume flow through the orifice as a function time for the API 521 wetted area and analytical fire models.

another pipe, which remains closed during the depressurization. The process conditions and inventory is the same as in our previous study given in Table 3. Initially, the pipes are filled completely with vapor.

In this case study, the average heat flux of 45 kW/m^2 is applied to the vessel. However, the total heat flux applied to the blowdown and vapor outlet pipes is treated differently. In the pipes, a global average initial heat flux of 45 kW/m^2 is applied but a peak initial flux of 120 kW/m^2 is applied on 0.1% of the area. Table 5 summarizes the dimensions in each of the individual vessel and pipes.

Fig. 11 shows the pressure profiles for the case of the vessel with piping and the case of a single vessel. Both systems depressurize at the same rate because the volume of the pipes are relatively small. Fig. 12 shows the vapor zone wall temperature of the vessel and pipes. Because the pipe walls are not as thick as the vessel wall, the vapor zones of the pipes heat up much faster than the vapor zone of a vessel. Additionally, as expected, the temperature rises in the pipes exposed to the peak flux of 120 kW/m^2 are much more rapid than the temperature rise of the vessel exposed to the average flux of 45 Kw/m^2. However, the pipe connected to the blowdown orifice heats up much less than the pipe connected with the blocked vapor outlet even though both pipes were exposed to peak flux of 120 kW/m^2. This is due to the fact that the gas velocity in the pipe connected to the blowdown orifice is much higher than the gas velocity in the pipe connected to the blocked vapor outlet. This results in higher internal convective heat transfer to the vapor going out of the orifice. Hence, the vapor wall of this pipe does not heat up as rapidly as that of the pipe connected to the blocked vapor outlet. Another observation that can be made from Fig. 12 is that for the pipe connected with the blocked vapor outlet, the peak wall temperature flattens out after 400 s. In this region, the heat absorbed by the vessel wall from the external fire is the same as the heat transfer to the inventory of the vessel.

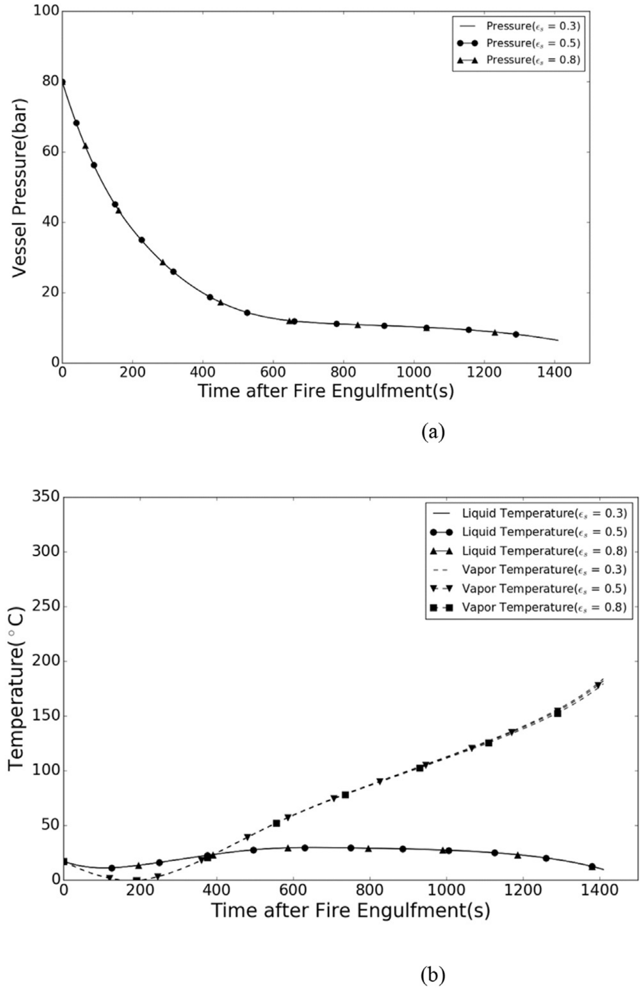

Fig. 8. S13 depressurization case (20% liquid inventory by vol.): (a) Vessel pressure and (b) liquid and vapor temperatures as a function of time for different surface emissivities with an initial fire heat flux of 45 kW/m^2.

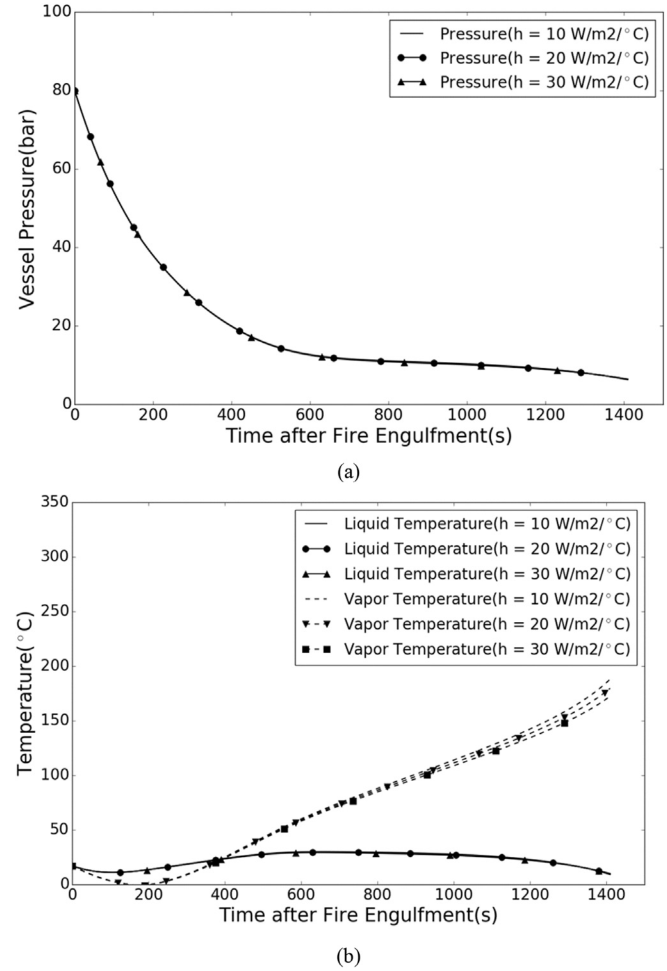

Fig. 9. S13 depressurization case (20% liquid inventory by vol.): (a) Vessel pressure and (b) liquid and vapor temperatures as a function of time for different external heat transfer coefficients with initial fire heat flux of 45 kW/m^2.

Although not performed in this study, Salater et al. (2002) and Scandpower Risk Management AS (2004) discuss how the wall temperature data obtained using the peak flux can be used to determine material failure. As the wall temperature in the vapor zone rises, there is thermal weakening of the vessel due to a loss of ultimate tensile strength (UTS) of the material. If the temperature-dependent data of the UTS of the material is available, then the UTS can be compared with the actual calculated stress in the pipe to verify when this mechanical failure will occur. Scandpower Risk Management AS (2004) provide details on the required safety factors, wear and tear, and other mechanical loading effects that need to be considered when embarking on this type of analysis.

As in the previous section, the effects of the surface emissivity and external heat transfer coefficients on the wall temperature profiles of the pipes that are exposed to peak flux are investigated. The fire temperature is calculated from Eq. (2) such that the initial local peak heat flux is 120 kW/m^2. Fig. 13(a) shows the wall temperature profiles in the vapor zone for the blocked vapor outlet pipe exposed to the peak flux for three different values of the surface emissivity (0.3, 0.5 and 0.8). As the surface emissivity decreases, the final wall temperature increases significantly. Conversely, varying the heat transfer coefficient has a smaller impact on the final wall temperature. As shown in Fig. 13(b), the wall temperature profiles in the vapor zone do not significantly change and are nearly identical in the initial period less than 200 s for three different heat transfer coefficients (10, 20, and 30 W/m^2/C).

As previously shown, for a single vessel, neither the surface emissivity nor the external heat transfer coefficient has strong effects on the pressure profile, vapor and liquid temperature profiles, and wall temperatures. However, in the associated piping with a local peak heat flux, the effect of surface emissivity on wall temperature can be significant. If the surface emissivity is varied, then Eq. (3) shows that the reduction of the heat flux will vary as the 4th power of wall temperature. However, if the external heat transfer coefficient is varied, then Eq. (3) shows that the reduction of the heat flux will vary linearly with wall temperature. Fig. 14 shows the decrease of the heat flux as a percentage of the initial peak flux (120 kW/m^2) with the vessel wall temperature for different surface emissivity values and for different external heat transfer coefficients. As shown, the differences in the heat flux are not significant until the wall temperature reaches approximately 500–600 C. In a vessel containing hydrocarbon liquid, the liquid inventory or the wetted wall will never reach this temperature because it is significantly higher than the bubble point of typical hydrocarbon liquids. Because the liquid inside of the vessel will absorb most of the heat from the fire, varying surface emissivity has no effect on the pressure profile, vapor and liquid temperatures, and wall temperatures. However, in the portion of the vapor outlet pipe where the peak heat flux of 120 kW/m^2 is applied, the wall

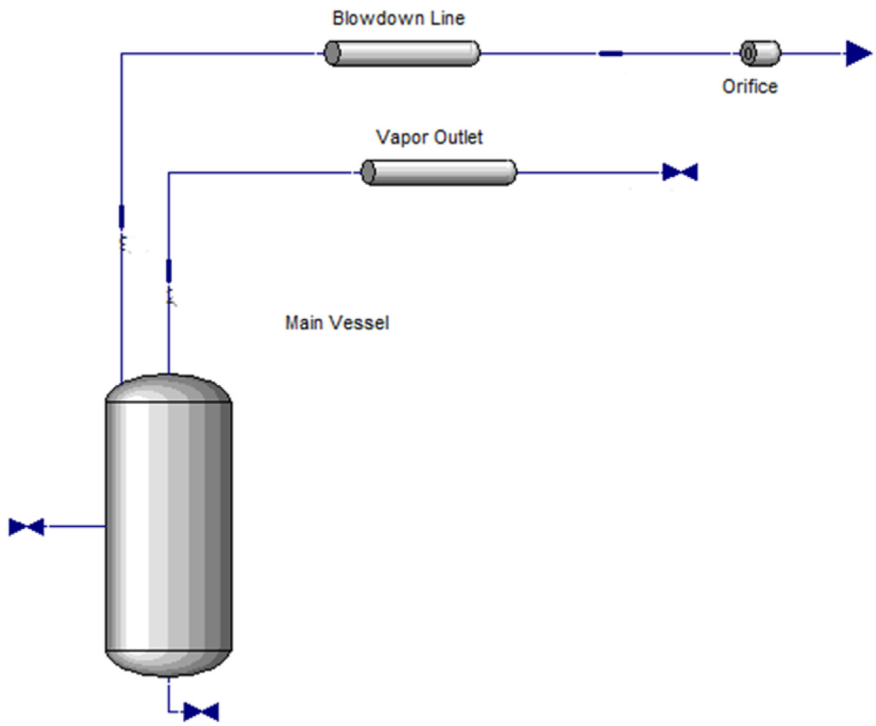

Fig. 10. Schematic diagram of the depressurization system where the vessel is connected to pipes in the outlet line and the blowdown line.

Table 5
Dimensions of individual vessel and pipes.

Parameters	Vessel	Pipe (Blocked Outlet)	Pipe (Blowdown Line)
Vessel Volume (m^3)	2.73		
Diameter	1.13 m	100 mm	100 mm
Pipe Length		5 m	5 m
Head Type	Dished	–	–
Cylindrical Wall Thickness (mm)	59 mm	10 mm	10 mm
Head Wall thickness (mm)	50	–	–
Initial Liquid Amount	20%	0%	0%
Area Exposed to Global Average Heat Flux (45 kW/m^2)	100%	99.9%	99.9%
Area Exposed to Peak Average Heat Flux (120^2)	0%	0.1%	0.1%
Composition	C1: 66.5%		
	C2: 3.5%		
	C3: 30%		
Final Time (s)	1500		
Orifice size(mm)	10		

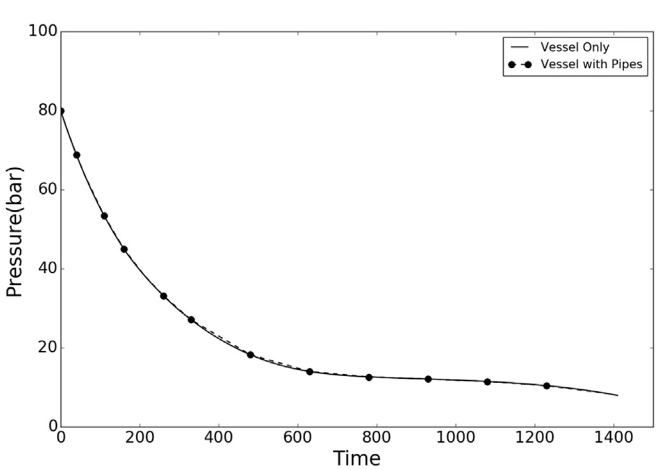

Fig. 11. Effect of the connected piping on the pressure in the system.

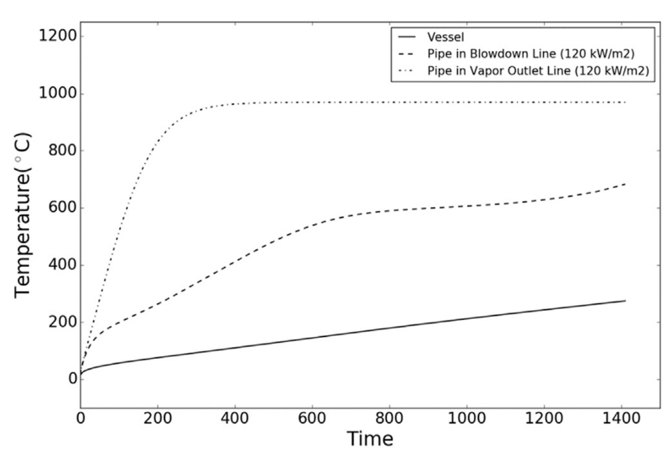

Fig. 12. S13 depressurization case (20% liquid inventory by vol.): Wall temperature at the location of the peak flux (120 kW/m^2) as a function of time.

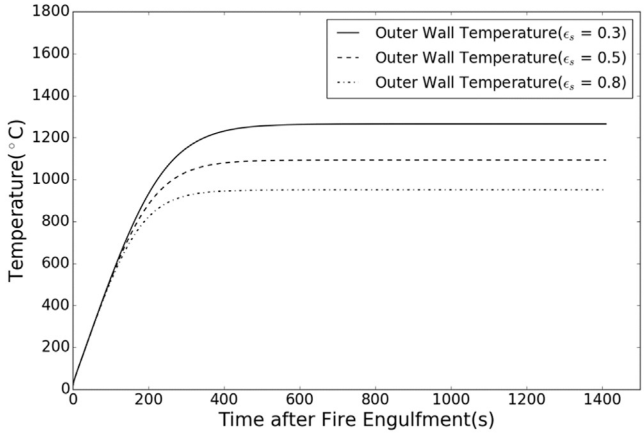

(a)

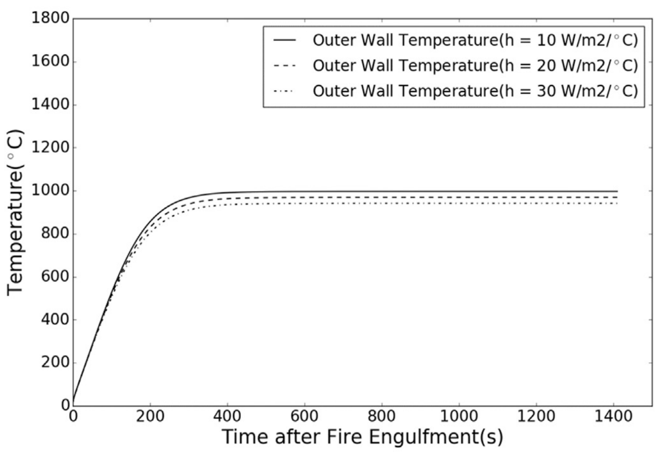

(b)

Fig. 13. Wall temperature at the location of the peak heat flux in the blocked vapor outlet line as a function of time for different (a) surface emissivities and (b) external heat transfer coefficients with an initial absorbed heat flux of 120 kW/m^2.

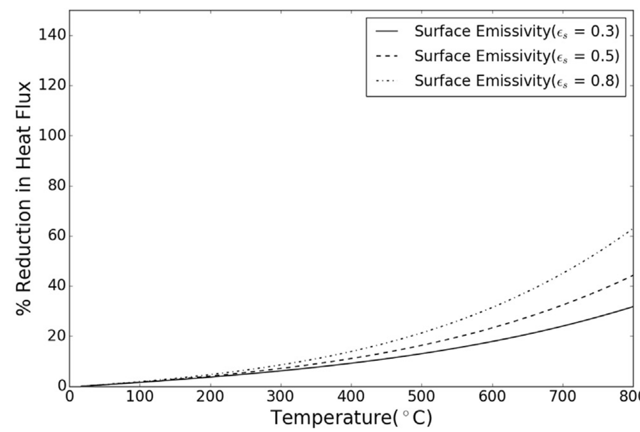

(a)

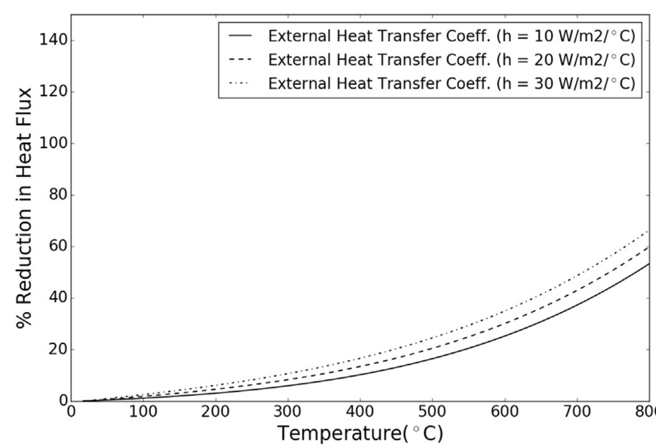

(b)

Fig. 14. Percentage reduction in the heat flux as a function of wall temperature for different (a) surface emissivities and (b) external heat transfer coefficients for an initial heat flux of 120 kW/m^2.

temperature goes well beyond 500–600C and as a result the wall temperature increase significantly. Lower emissivity leads to lower re-emitted heat flux from the vessel, and therefore higher absorbed heat flux by the equipment wall. This leads to a higher and thus more conservative wall temperature predictions.

6. Conclusion

Predictions using the analytical fire equation from API 521 with the BLOWDOWN Technology in Aspen HYSYS compared well with available experimental data from fire engulfment studies of LPG tanks. By using the proper amount of heat flux, the pressure profiles and vapor and liquid temperature profiles were consistent with experimental data from Moodie et al. (1988). In addition, results from comparison studies of different fire models show that the pressure profiles using the empirical wetted area equation compares well with the analytical equation provided that the initial heat flux used in the analytical fire model is the same as the heat flux directly applied to fluid in the wetted area model. However, the wetted area model does not account for the sensible heating of the vapor and the resultant temperature increase of the fluid downstream of the orifice. This leads to marginally lower volumetric flow predictions in the downstream flare networks.

Although the API 521 analytical equation has several parameters that are difficult to obtain, it was shown that only the surface emissivity and heat transfer coefficient affect the absorbed heat flux with time. In a vessel undergoing depressurization, the surface emissivity does not affect the predictions for either the pressure or fluid phase (vapor and liquid) temperatures inside of the vessel. This is because the wall temperature never gets high enough to cause a significant difference in the absorbed heat flux. However, it was shown that the wall temperature in a vapor-filled pipe exposed to a local peak heat flux will increase significantly with a decrease in surface emissivity. In addition, the flow in the vapor-filled pipe affects the wall temperature significantly because of the enhanced heat transfer between the flowing vapor and the pipe wall. As a result, in depressurization systems, the wall temperature of pipes with significant flow, such as the blowdown line, do not get as high as that of pipes connected to blocked outlets with lower flows. In both the vessel and pipe, varying the external heat transfer coefficient was found to exert an insignificant effect. From these observations, it can be concluded that the absorbed heat flux at the initial time is the key factor when sizing an orifice in a system exposed to fire. But when extending the analysis to material failure using a local peak heat flux, lower surface emissivity values lead to more conservative results for wall temperatures.

When analyzing a fire scenario, safety engineers often design a blowdown valve by determining the orifice size required to reduce the pressure to 50% of the design pressure within 15 min. By using the tools and methods in this study, wall temperatures in the vessel and piping can be calculated more accurately during blowdown and therefore the orifice size can be based on a stress analysis rather than the traditional “15 min rule”. Evaluating the pressure and thermal stress profiles with a comparison to the yield strength of the material will allow engineers to determine the minimum blowdown rate that can avoid rupture. It should also be pointed out that this study still assumes that the vessel is engulfed by the fire. Further investigations are required to estimate the heat flux in the Stefan-Boltzmann equations for a fire distant to the process equipment, which would require a full three-dimensional study of the heat transfer inside the process equipment.

Acknowledgements

The authors are grateful to Dr. Graham Saville and Professor Stephen Richardson, formerly of Imperial College London, for invaluable discussions.

References

Anderson, C., Townsend, W., Zook, J., Cowgill, G., 1974. The Effects of a Fire Environment on a Rail Tank Car Filled with LPG. Rept No FRA-OR&D. US Dept of Trans, p. 75, 31.
ANSI/API Standard 521 6th Edition, 2014. Pressure-Relieving and Depressuring Systems.
Balke, C., Heller, W., Konersmann, R., Ludwig, J., 1999. Study of the Failure Limits of a Railway Tank Car Filled with Liquefied Petroleum Gas Subjected to an Open Pool Fire Test. BAM project, p. 3215.
Haque, M.A., Richardson, S.M., Saville, G., 1992a. Blowdown of pressure vessels. I. Computer model. Trans. IChemE, Part B, Proc. Safe Env. Prot. 70 (B1), 3–9.
Haque, M.A., Richardson, S.M., Saville, G., Chamberlain, G., Shirvill, L., 1992b. Blowdown of pressure vessels. II. Experimental validation of computer model and case studies. Trans. IChemE, Part B, Proc. Safe Env. Prot. 70 (B1), 10–17.
Ludwig, J., Heller, W., 1999. Fire Test with a Propane Tank Car. BAM Test Report III.2/9907.
Moodie, K., Billinge, K., Cutler, D.P., April 1985. The fire engulfment of LPG. storage tanks'. I. Chem. E. Symp. Assess. Control Major Hazards. DMIST.
Moodie, K., Cowley, L.T., Denny, R.B., Small, L.M., Williams, I., 1988. Fire engulfment tests on a 5 tonne LPG tank. J. Hazard. Mater. 20, 55–71.
Mahgerefteh, H., Falope, G.B., Oke, A.O., 2002. Modeling blowdown of cylindrical vessels under fire attack. AIChE J. 48 (2), 401–410.
Melhem, G.A., Gaydos, D., 2015. Properly calculate vessel and piping wall temperatures during depressuring and relief. Process Saf. Prog. 34 (1), 64–71.
Roberts, T.A., Buckland, I., Shirvill, L.C., Lowesmith, B.J., Salater, P., 2004. Design and protection of pressure systems to withstand severe fires. Process Saf. Environ. Prot. 82 (2), 89–96.
Salater, P., Overaa, S.J., Kjensjord, E., 2002. Size depressurization and relief devices for pressurized segments exposed to fire. Chem. Eng. Prog. 98 (9), 38–45.
Scandpower Risk Management AS, 2004. Guidelines for Protection of Pressurized Systems Exposed to Fire. Scandpower, AS, Norway.
Zamejc, E., 2014. API Standard 521 new alternative method to evaluate fire relief for pressure relief device sizing and depressuring system design. J. Loss Prev. Process Industries 27, 21–31.